IEEE Access
Multidisciplinary : Rapid Review : Open Access Journal

Received September 30, 2020, accepted October 19, 2020, date of publication October 29, 2020, date of current version November 12, 2020.

Digital Object Identifier 10.1109/ACCESS.2020.3034696

An Artificial Anisotropy Four-Step HIE-FDTD Method With Lower Numerical Dispersion Error

YONG-DAN KONG, (Member, IEEE), CHU-BIN ZHANG, HONG-YU ZHANG, AND QING-XIN CHU, (Fellow, IEEE)
School of Electronic and Information Engineering, South China University of Technology, Guangzhou 510640, China

Corresponding author: Yong-Dan Kong (eeydkong@scut.edu.cn)

This work was supported in part by the National Natural Science Foundation of China under Grant 61171029, Grant 61671207, and Grant 61901176, in part by the Fundamental Research Funds for the Central Universities under Grant 2017ZD055 and Grant 2020ZYGXZR019, and in part by the Guangzhou Science and Technology Project under Grant 202002030118.

ABSTRACT In this article, by introducing artificial anisotropic (AA) parameters in the four-step hybrid implicit-explicit finite-difference time domain (HIE-FDTD) method, an AA four-step HIE-FDTD method is proposed, which can reduce the numerical dispersion error and improve the computational accuracy. Firstly, the Maxwell's matrix equation is decomposed into four sub-matrix equations by using the split-step scheme, and artificial anisotropy parameters are introduced, then the proposed AA four-step HIE-FDTD is obtained. Furthermore, the stability analysis of the AA four-step HIE-FDTD method shows that the stability condition of the proposed method is closed to the original four-step HIE-FDTD method. Next, the numerical dispersion characteristics of the proposed method are analyzed and compared with other HIE-FDTD methods. The results show that the numerical dispersion error of the proposed method is significantly reduced compared with the four-step HIE-FDTD method. Finally, the performance of the proposed method is further verified by the numerical simulation. Numerical results show that the proposed method has lower numerical dispersion error and higher computational accuracy than that of the four-step HIE-FDTD method.

INDEX TERMS Finite-difference time domain (FDTD), hybrid implicit-explicit (HIE), artificial anisotropy (AA), numerical dispersion.

I. INTRODUCTION

The finite-difference time-domain (FDTD) method [1] is one of the most widely used electromagnetic numerical calculation methods, but the Courant-Friedrichs-Lewy (CFL) stability condition [2] limits the computational efficiency of the method in the miniaturized and complicated electromagnetic field problems.

In order to remove the limitation of the CFL stability condition, the alternating-direction implicit (ADI) FDTD method [3], [4] has been proposed. The ADI-FDTD method uses the implicit method to solve iteratively, so that the time step value of the method is no longer controlled by the spatial grid size, then larger time steps can be used to improve the computational efficiency. Following the ADI-FDTD method, some other unconditionally stability methods have been presented, such as the Crank-Nicolson (CN) FDTD method [5], the split-step (SS) FDTD method [6]–[8], the locally-one-dimensional (LOD) FDTD method [9]–[11].

In addition, considering the electromagnetic field problems associated with fine structures in one or two directions, conditionally stable FDTD methods, such as the hybrid explicit-implicit FDTD (HIE-FDTD) method [12], [13] and the weakly conditionally stable FDTD (WCS-FDTD) method [14] have also been presented. In order to further increase the value of the time step of the HIE-FDTD method, a new 2D HIE-FDTD method has been proposed [15], [16], and the maximum time step is taken as $2\Delta x/c$, compared with the original 2D HIE-FDTD method ($\Delta x/c$), the time step is increased significantly. Then, Wang *et al.* proposed a new 3D one-step leapfrog HIE-FDTD method in [17] with a CFL stability condition of $\Delta t < \Delta x/c$ & $\Delta t < \Delta z/c$

The associate editor coordinating the review of this manuscript and approving it for publication was Jon Atli Benediktsson.

(suppose the fine grid only in the y-direction), and it's the time step value can be increased compared with the original 3D HIE-FDTD method ($\Delta t \leq 1/(c\sqrt{1/\Delta x^2 + 1/\Delta z^2})$). In addition, Wang *et al.* proposed a weaker 3D HIE-FDTD method in [18], which increases the maximum value of the time step to twice as the original HIE-FDTD algorithm ($\Delta t \leq 2/(c\sqrt{1/\Delta x^2 + 1/\Delta z^2})$). Furthermore, we presented a four-step HIE-FDTD method with weaker CFL stability condition ($\Delta t \leq 2\Delta x/c$ and $\Delta t \leq 2\Delta z/c$) in [19].

However, whether unconditionally stable FDTD methods or conditionally stable FDTD methods, the numerical dispersion error increases as the increase of time step size. In order to reduce the numerical dispersion error, by introducing an artificial anisotropic (AA) method, a low computational cost correction method for FDTD method is proposed [20]. Recently, this optimization method has been applied to the ADI-FDTD method [21], [22], the WCS-FDTD method [23] and the HIE-FDTD methods [24]–[26].

In this article, based on the four-step HIE-FDTD method [19], combined with the an artificial anisotropic (AA) method, a novel AA four-step HIE-FDTD method with lower numerical dispersion error is proposed. In Section II, the formulation of the AA four-step HIE-FDTD method is given. the Maxwell's matrix equation is decomposed into four sub-matrix equations by using the split-step scheme, and AA parameters are introduced simultaneously. In Section III, the numerical stability of the AA four-step HIE-FDTD method is analyzed. In Section IV, the numerical dispersion characteristics of the proposed method are analyzed, and compared with the traditional FDTD method, the ADI-FDTD method, the HIE-FDTD method, the one-step leapfrog HIE-FDTD method and the four-step HIE-FDTD method. Finally, in Section V, to testify the efficiency and accuracy of the AA four-step HIE-FDTD method, numerical simulation results of the cavities are given.

II. FOMULATION

In a linear, isotropic, lossless and non-dispersive medium, by introducing the artificial anisotropy parameters diag$\{\varepsilon_x, \varepsilon_y, \varepsilon_z\}$ and diag$\{\mu_x, \mu_y, \mu_z\}$, the 3-D Maxwell's matrix can be written as

$$\frac{\partial \vec{u}}{\partial t} = [R]\,\vec{u} \tag{1}$$

where $\vec{u} = \left[E_x, E_y, E_z, H_x, H_y, H_z\right]^T$, and

$$[R] = \begin{bmatrix} 0 & 0 & 0 & 0 & -\frac{1}{\varepsilon}\frac{\partial}{\partial z}\frac{1}{\varepsilon_z} & \frac{1}{\varepsilon}\frac{\partial}{\partial y}\frac{1}{\varepsilon_y} \\ 0 & 0 & 0 & \frac{1}{\varepsilon}\frac{\partial}{\partial z}\frac{1}{\varepsilon_z} & 0 & -\frac{1}{\varepsilon}\frac{\partial}{\partial x}\frac{1}{\varepsilon_x} \\ 0 & 0 & 0 & -\frac{1}{\varepsilon}\frac{\partial}{\partial y}\frac{1}{\varepsilon_y} & \frac{1}{\varepsilon}\frac{\partial}{\partial x}\frac{1}{\varepsilon_x} & 0 \\ 0 & -\frac{1}{\mu}\frac{\partial}{\partial z}\frac{1}{\mu_z} & \frac{1}{\mu}\frac{\partial}{\partial y}\frac{1}{\mu_y} & 0 & 0 & 0 \\ \frac{1}{\mu}\frac{\partial}{\partial z}\frac{1}{\mu_z} & 0 & -\frac{1}{\mu}\frac{\partial}{\partial x}\frac{1}{\mu_x} & 0 & 0 & 0 \\ -\frac{1}{\mu}\frac{\partial}{\partial y}\frac{1}{\mu_y} & \frac{1}{\mu}\frac{\partial}{\partial x}\frac{1}{\mu_x} & 0 & 0 & 0 & 0 \end{bmatrix}$$

ε and μ are the electric permittivity and the magnetic permeability, respectively. To simplify the calculation, here $\varepsilon_\alpha = \mu_\alpha (\alpha = x, y, z)$.

In this article, the fine structure is taken in the y direction as an example. By using the implicit form for the y direction and explicit form for the x and z directions, thereby decomposing the matrix $[R]$ into four sub-matrices of $[M]/2$, $[N]/2$, $[M]/2$, and $[N]/2$, and

$$[M] = \begin{bmatrix} 0 & 0 & 0 & 0 & 0 & \frac{\partial}{\varepsilon\varepsilon_y\partial y} \\ 0 & 0 & 0 & 0 & 0 & -\frac{\partial}{\varepsilon\varepsilon_x\partial x} \\ 0 & 0 & 0 & 0 & \frac{\partial}{\varepsilon\varepsilon_x\partial x} & 0 \\ 0 & \frac{\partial}{\mu\mu_z\partial z} & 0 & 0 & 0 & 0 \\ -\frac{\partial}{\mu\mu_z\partial z} & 0 & 0 & 0 & 0 & 0 \\ \frac{\partial}{\mu\mu_y\partial y} & 0 & 0 & 0 & 0 & 0 \end{bmatrix}$$

$$[N] = \begin{bmatrix} 0 & 0 & 0 & 0 & -\frac{\partial}{\varepsilon\varepsilon_z\partial z} & 0 \\ 0 & 0 & 0 & \frac{\partial}{\varepsilon\varepsilon_z\partial z} & 0 & 0 \\ 0 & 0 & 0 & -\frac{\partial}{\varepsilon\varepsilon_y\partial y} & 0 & 0 \\ 0 & 0 & -\frac{\partial}{\mu\mu_y\partial y} & 0 & 0 & 0 \\ 0 & 0 & \frac{\partial}{\mu\mu_x\partial x} & 0 & 0 & 0 \\ 0 & -\frac{\partial}{\mu\mu_x\partial x} & 0 & 0 & 0 & 0 \end{bmatrix}$$

Then, (1) can be written as

$$\frac{\partial \vec{u}}{\partial t} = \frac{[M]}{2}\vec{u} + \frac{[N]}{2}\vec{u} + \frac{[M]}{2}\vec{u} + \frac{[N]}{2}\vec{u} \tag{2}$$

Furthermore, (2) is decomposed into four submatrix equations using the split-step scheme, which is shown as follows

$$\text{sub-step 1:} \quad \left([I] - \frac{\Delta t}{4}[M]\right)\vec{u}^{n+1/4} = \left([I] + \frac{\Delta t}{4}[N]\right)\vec{u}^{n} \tag{3a}$$

$$\text{sub-step 2:}\quad \left([I]-\frac{\Delta t}{4}[N]\right)\vec{u}^{n+2/4} = \left([I]+\frac{\Delta t}{4}[M]\right)\vec{u}^{n+1/4} \tag{3b}$$

$$\text{sub-step 3:}\quad \left([I]-\frac{\Delta t}{4}[M]\right)\vec{u}^{n+3/4} = \left([I]+\frac{\Delta t}{4}[N]\right)\vec{u}^{n+2/4} \tag{3c}$$

$$\text{sub-step 4:}\quad \left([I]-\frac{\Delta t}{4}[N]\right)\vec{u}^{n+1} = \left([I]+\frac{\Delta t}{4}[M]\right)\vec{u}^{n+3/4} \tag{3d}$$

In sub-step 1, by performing the central difference approximation on the time derivative and the spatial derivative in (3a), and the calculation formulas can be obtained as follows

$$\begin{aligned} &E_x|_{i+1/2,j,k}^{n+1/4} - \frac{\Delta t}{4\varepsilon\varepsilon_y\Delta y}\left(H_z|_{i+1/2,j+1/2,k}^{n+1/4} - H_z|_{i+1/2,j-1/2,k}^{n+1/4}\right) \\ &= E_x|_{i+1/2,j,k}^{n} - \frac{\Delta t}{4\varepsilon\varepsilon_z\Delta z}\left(H_y|_{i+1/2,j,k+1/2}^{n}\right. \\ &\quad \left. - H_y|_{i+1/2,j,k-1/2}^{n}\right) \end{aligned} \tag{4a}$$

$$\begin{aligned} &E_y|_{i,j+1/2,k}^{n+1/4} + \frac{\Delta t}{4\varepsilon\varepsilon_x\Delta x}\left(H_z|_{i+1/2,j+1/2,k}^{n+1/4} - H_z|_{i-1/2,j+1/2,k}^{n+1/4}\right) \\ &= E_y|_{i,j+1/2,k}^{n} + \frac{\Delta t}{4\varepsilon\varepsilon_z\Delta z}\left(H_x|_{i,j+1/2,k+1/2}^{n}\right. \\ &\quad \left. - H_x|_{i,j+1/2,k-1/2}^{n}\right) \end{aligned} \tag{4b}$$

$$\begin{aligned} &E_z|_{i,j,k+1/2}^{n+1/4} - \frac{\Delta t}{4\varepsilon\varepsilon_x\Delta x}\left(H_y|_{i+1/2,j,k+1/2}^{n+1/4} - H_y|_{i-1/2,j,k+1/2}^{n+1/4}\right) \\ &= E_z|_{i,j,k+1/2}^{n} - \frac{\Delta t}{4\varepsilon\varepsilon_y\Delta y}\left(H_x|_{i,j+1/2,k+1/2}^{n}\right. \\ &\quad \left. - H_x|_{i,j-1/2,k+1/2}^{n}\right) \end{aligned} \tag{4c}$$

$$\begin{aligned} &H_x|_{i,j+1/2,k+1/2}^{n+1/4} - \frac{\Delta t}{4\mu\mu_z\Delta z}\left(E_y|_{i,j+1/2,k+1}^{n+1/4} - E_y|_{i,j+1/2,k}^{n+1/4}\right) \\ &= H_x|_{i,j+1/2,k+1/2}^{n} - \frac{\Delta t}{4\mu\mu_y\Delta y}\left(E_z|_{i,j+1,k+1/2}^{n}\right. \\ &\quad \left. - E_z|_{i,j,k+1/2}^{n}\right) \end{aligned} \tag{4d}$$

$$\begin{aligned} &H_y|_{i+1/2,j,k+1/2}^{n+1/4} + \frac{\Delta t}{4\mu\mu_z\Delta z}\left(E_x|_{i+1/2,j,k+1}^{n+1/4} - E_x|_{i+1/2,j,k}^{n+1/4}\right) \\ &= H_y|_{i+1/2,j,k+1/2}^{n} + \frac{\Delta t}{4\mu\mu_x\Delta x}\left(E_z|_{i+1,j,k+1/2}^{n}\right. \\ &\quad \left. - E_z|_{i,j,k+1/2}^{n}\right) \end{aligned} \tag{4e}$$

$$\begin{aligned} &H_z|_{i+1/2,j+1/2,k}^{n+1/4} - \frac{\Delta t}{4\mu\mu_y\Delta y}\left(E_x|_{i+1/2,j+1,k}^{n+1/4} - E_x|_{i+1/2,j,k}^{n+1/4}\right) \\ &= H_z|_{i+1/2,j+1/2,k}^{n} - \frac{\Delta t}{4\mu\mu_x\Delta x}\left(E_y|_{i+1,j+1/2,k}^{n}\right. \\ &\quad \left. - E_y|_{i,j+1/2,k}^{n}\right) \end{aligned} \tag{4f}$$

By observing the formulas (4a) and (4f), the electric field component $E_x|_{i+1/2,j,k}^{n+1/4}$ and the magnetic field component $H_z|_{i+1/2,j+1/2,k}^{n+1/4}$ are coupled to each other, and (4f) is substituted into (4a) to obtain the triangular matrix equation about $E_x|_{i+1/2,j,k}^{n+1/4}$ as follows

$$\begin{aligned} &\left(1+\frac{\Delta t^2}{8\varepsilon_y^2\Delta y^2}\right)E_x|_{i+1/2,j,k}^{n+1/4} - \frac{\Delta t^2}{16\varepsilon_y^2\Delta y^2} \\ &\quad\times\left(E_x|_{i+1/2,j+1,k}^{n+1/4} + E_x|_{i+1/2,j-1,k}^{n+1/4}\right) \\ &= E_x|_{i+1/2,j,k}^{n} + \frac{\Delta t}{4\varepsilon_y\Delta y}\left(H_z|_{i+1/2,j+1/2,k}^{n} - H_z|_{i+1/2,j-1/2,k}^{n}\right) \\ &\quad - \frac{\Delta t^2}{16\varepsilon_x\varepsilon_y\Delta x\Delta y}\left(E_y|_{i+1,j+1/2,k}^{n} - E_y|_{i+1,j-1/2,k}^{n}\right. \\ &\quad \left. - E_y|_{i,j+1/2,k}^{n} + E_y|_{i,j-1/2,k}^{n}\right) \\ &\quad - \frac{\Delta t}{4\varepsilon_z\Delta z}\left(H_y|_{i+1/2,j,k+1/2}^{n} - H_y|_{i+1/2,j,k-1/2}^{n}\right) \end{aligned} \tag{5}$$

By solving the triangular matrix equation (5), the electric field component $E_x|_{i+1/2,j,k}^{n+1/4}$ can be solved, and the remaining field components can be solved by the explicit iteration. The solutions of sub-step 2, 3, and 4 is similar to sub-step 1, which are not shown here.

III. NUMERICAL STABILITY ANALYSIS

The Fourier method is used to analyze the numerical stability of the AA four-step HIE-FDTD method. The expression of the AA four-step HIE-FDTD algorithm in a complete time step is shown as follows

$$U^{n+1} = [\Lambda_2][\Lambda_1][\Lambda_2][\Lambda_1]U^n = [\Lambda]U^n \tag{6}$$

where $[\Lambda]$ is the growth matrix of the entire time step, $[\Lambda_1]$ and $[\Lambda_2]$ are the growth matrices of each sub-step. The expressions of $[\Lambda_1]$ and $[\Lambda_2]$ are as follows

$$[\Lambda_1] = \begin{bmatrix} \frac{4}{A'_y} & \frac{l_xl_y}{A'_y} & 0 & 0 & -\frac{2jl_z}{A'_y} & \frac{2jl_z}{A'_y} \\ \frac{l_xl_y}{A'_y} & 1-\frac{l_x^2}{A'_y} & 0 & \frac{jl_z}{2} & -\frac{jl_xl_yl_z}{2A'_y} & -\frac{2jl_x}{A'_y} \\ \frac{l_xl_z}{A'_y} & \frac{l_x^2l_yl_z}{4A'_y} & 1-\frac{l_x^2}{4} & -\frac{jl_y}{2} & -\frac{jl_xl_z^2}{2A'_y}+\frac{jl_x}{2} & \frac{jl_xl_yl_z}{2A'_y} \\ \frac{jl_xl_yl_z}{2A'_y} & \frac{jl_z}{2}-\frac{jl_x^2l_z}{2A'_y} & -\frac{jl_y}{2} & 1-\frac{l_z^2}{4} & \frac{l_xl_yl_z^2}{4A'_y} & \frac{l_xl_z}{A'_y} \\ -\frac{2jl_z}{A'_y} & -\frac{jl_xl_yl_z}{2A'_y} & \frac{jl_x}{2} & 0 & 1-\frac{l_z^2}{A'_y} & \frac{l_yl_z}{A'_y} \\ \frac{2jl_y}{A'_y} & -\frac{2jl_x}{A'_y} & 0 & 0 & \frac{l_yl_z}{A'_y} & \frac{4}{A'_y} \end{bmatrix}$$

$$[\Lambda_2] = \begin{bmatrix} 1-\frac{l_z^2}{4} & \frac{l_xl_yl_z^2}{4A'_y} & \frac{l_xl_z}{A'_y} & -\frac{jl_xl_yl_z}{2A'_y} & \frac{jl_x^2l_z}{2A'_y}-\frac{jl_z}{2} & \frac{jl_y}{2} \\ 0 & 1-\frac{l_z^2}{A'_y} & \frac{l_yl_z}{A'_y} & \frac{2jl_z}{A'_y} & \frac{jl_xl_yl_z}{2A'_y} & -\frac{jl_x}{2} \\ 0 & \frac{l_yl_z}{A'_y} & \frac{4}{A'_y} & -\frac{2jl_y}{A'_y} & \frac{2jl_x}{A'_y} & 0 \\ 0 & \frac{2jl_z}{A'_y} & -\frac{2jl_y}{A'_y} & \frac{4}{A'_y} & \frac{l_xl_y}{A'_y} & 0 \\ -\frac{jl_z}{2} & \frac{jl_xl_yl_z}{2A'_y} & \frac{2jl_x}{A'_y} & \frac{l_xl_y}{A'_y} & 1-\frac{l_x^2}{A'_y} & 0 \\ \frac{jl_y}{2} & \frac{jl_xl_z^2}{2A'_y}-\frac{jl_x}{2} & -\frac{jl_xl_yl_z}{2A'_y} & \frac{l_xl_z}{A'_y} & \frac{l_x^2l_yl_z}{4A'_y} & 1-\frac{l_x^2}{4} \end{bmatrix}$$

where $b = \Delta t/2\varepsilon$, $d = \Delta t/2\mu$, $\partial/\partial\alpha = jP_\alpha = -2j\sin(k_\alpha\Delta\alpha/2)/\Delta\alpha$, $r_\alpha^2 = bdP_\alpha^2$, $l_\alpha = r_\alpha/\varepsilon_\alpha$, $\alpha = x, y, z$, $A'_y = bdP_y^2/\varepsilon_y^2 + 1$.

To ensure that the algorithm remains stable during the iterative process, the modulus of the eigenvalues of the growth matrix must be less than or equal to 1, and the six eigenvalues of the matrix $[\Lambda]$ are calculated as follows

$$\lambda_1 = \lambda_2 = 1 \tag{7a}$$

$$\lambda_3 = \lambda_4 = \lambda_5^* = \lambda_6^* = \frac{C + j\sqrt{4E^2 - C^2}}{2E} \tag{7b}$$

where

$$C = \varepsilon_x^4\varepsilon_y^4\varepsilon_z^4\left(\begin{array}{l}\left(\frac{r_x^2}{\varepsilon_x^2}-4\right)\left(\frac{r_z^2}{\varepsilon_z^2}-4\right)\left(\frac{r_x^2}{\varepsilon_x^2}\left(\frac{r_z^2}{\varepsilon_z^2}-4\right)\right.\\ \left.-4\left(\frac{r_y^2}{\varepsilon_y^2}+\frac{r_z^2}{\varepsilon_z^2}\right)\right)+2\left(\frac{r_y^2}{\varepsilon_y^2}+4\right)^2\end{array}\right),$$

$$E = \varepsilon_x^4\varepsilon_y^4\varepsilon_z^4\left(\frac{r_y^2}{\varepsilon_x^2}+4\right)^2$$

When $|\lambda_3| = |\lambda_4| = |\lambda_5| = |\lambda_6| \le 1$, the AA four-step HIE-FDTD method will be stable. Then, $4E^2$-$C^2 \ge 0$ must be satisfied, and

$$4E^2 - C = \varepsilon_x^4\varepsilon_y^4\varepsilon_z^4 T_1T_2T_3 \tag{8}$$

where $T_1 = \left(\frac{r_z^2}{\varepsilon_z^2} - 4\right)$, $T_2 = \left(\frac{r_x^2}{\varepsilon_x^2} - 4\right)$, $T_3 = \left[4T_4 - \frac{r_x^2}{\varepsilon_x^2}T_1\right]$, $T_4 = \left(\frac{r_y^2}{\varepsilon_y^2} + \frac{r_z^2}{\varepsilon_z^2}\right)$.

Obviously, $T_4 \ge 0$ is always true. Assuming that T_1 and T_2 are both positive or negative, there are two cases. In case 1, if both T_1 and T_2 are positive, then $T_3 \ge 0$ cannot be guaranteed, and $4E^2$-$C^2 \ge 0$ also cannot be guaranteed. In case 2, if both T_1 and T_2 are negative, then $T_3 \ge 0$, and it can be guaranteed to ensure that $4E^2$-$C^2 \ge 0$. Therefore, case 2 satisfies the stable condition. In other words, when both T_1 and T_2 are negative, the AA four-step HIE-FDTD method is stable. Then, the stability condition of the AA four-step HIE-FDTD method can be obtained as

$$\Delta t \le \frac{2\varepsilon_x\Delta x}{c} \quad \& \quad \Delta t \le \frac{2\varepsilon_z\Delta z}{c} \tag{9}$$

Similarly, the stability condition of the four-step HIE-FDTD method can be obtained as $\Delta t \le 2\Delta x/c$ & $\Delta t \le 2\Delta z/c$ in [19]. Since the values of the artificial anisotropy parameters are close to 1, the stability condition of the proposed method is almost equal to that of the four-step HIE-FDTD method. Compared with the stability conditions of the HIE-FDTD method ($\Delta t \le 1/(c\sqrt{1/\Delta x^2 + 1/\Delta z^2})$), the leapfrog HIE-FDTD method ($\Delta t < \Delta x/c$ & $\Delta t < \Delta z/c$) and the weaken HIE-FDTD method ($\Delta t \le 2/(c\sqrt{1/\Delta x^2 + 1/\Delta z^2})$), the stability condition of the proposed AA four-step HIE-FDTD method is more weaker.

IV. NUMERICAL DISPERSION ANALYSIS

The dispersion relation expression of the AA four-step HIE-FDTD method can be obtained as

$$\begin{aligned}\cos(\omega\Delta t) &= \frac{C}{2E}\\ &= \frac{\left(\frac{r_x^2}{\varepsilon_x^2}-4\right)\left(\frac{r_z^2}{\varepsilon_z^2}-4\right)\left(\begin{array}{c}\frac{r_x^2}{\varepsilon_x^2}\left(\frac{r_z^2}{\varepsilon_z^2}-4\right)\\ -4\left(\frac{r_y^2}{\varepsilon_y^2}+\frac{r_z^2}{\varepsilon_z^2}\right)\end{array}\right)+2\left(\frac{r_y^2}{\varepsilon_y^2}+4\right)^2}{2\left(\frac{r_y^2}{\varepsilon_y^2}+4\right)^2}\end{aligned} \tag{10}$$

Then, the artificial anisotropy parameters can be obtained by the dispersion relation expression. The effect of the artificial anisotropy parameters is to make the normalized numerical phase velocity $A = v_p/c$ approach to 1. First, assuming $A = 1$, the initial values of the parameters, ε_x^0, ε_y^0 and ε_z^0 can be obtained by the dispersion relation of (10). Second, the initial values ε_x^0, ε_y^0 and ε_z^0 are substituted into (10), and the maximum value A_{max} can be obtained by scanning θ and φ in the range of (0, 90°). Finally, the corrected value A is obtained by using the modified formula $A = 1 - (|A_{max} - 1|)/2$. The final optimization parameters ε_x, ε_y and ε_z are calculated by the corrected value A substituting into (10).

Next, the numerical dispersion characteristics of the proposed method both in the uniform grid system and non-uniform grid system are analyzed respectively. The influences of different parameters on the numerical dispersion characteristics of the algorithm are also analyzed.

Figs. 1 and 2 are numerical dispersion characteristics analysis of the proposed AA four-step HIE-FDTD method in the uniform grid system. Here, $\Delta x = \Delta y = \Delta z = \lambda/37.1$, and the number of cells per wavelength (CPW) is 37.1, and CFL numbers (CFLN) is defined as $\Delta t/\Delta t_0$, where $\Delta t_0 = 1\Big/\left(c\sqrt{1/\Delta x^2 + 1/\Delta y^2 + 1/\Delta z^2}\right)$, and $\Delta t\Delta t$ is the time step size adopted by different FDTD methods, and the CFLN is 1.1547. The normalized numerical phase velocity error (NNPVE) is defined as $|1 - v_p/c| \times 100\%$. The optimized parameters of the proposed method can be calculated as $\varepsilon_x = \varepsilon_z = 0.9992$ and $\varepsilon_y = 0.9988$.

Fig. 1 shows the comparison of Maximum NNPVE versus propagation angle θ of the six methods. Fig. 2 presents the NNPVE with θ and φ for the FDTD method, the four-step HIE-FDTD method and the AA four-step HIE-FDTD method. As reflected in Figs. 1 and 2, some results can be found. (1) For the value of θ ranging from 0 to 180°, the maximum NNPVE of the AA four-step HIE-FDTD algorithm is lower than those of the other four methods except the traditional FDTD method; (2) For the six methods, the maximum NNPVE reaches the maximum value when θ is 90°. The maximum NNPVE of the four-step HIE-FDTD method is 0.1458%, and the maximum value of the AA four-step

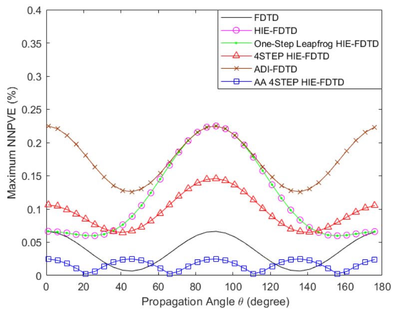

FIGURE 1. **Maximum NNPVE versus θ of the six methods with CPW = 37.1 and CFLN = 1.1547 in the uniform grid system.**

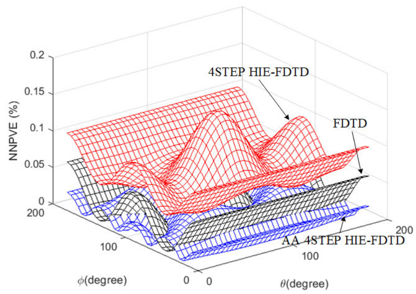

FIGURE 2. **NNPVE versus θ and φ of the three methods with CPW = 37.1 and CFLN = 1.1547 in the uniform grid system.**

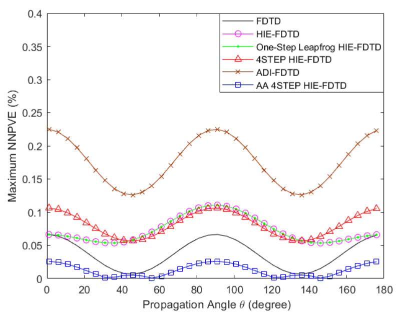

FIGURE 3. **Maximum NNPVE versus θ of the six methods with CPW = 37.1 and CFLN = 3.4647 in the nonuniform grid system.**

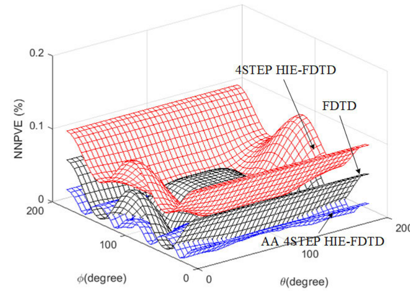

FIGURE 4. **NNPVE versus θ and φ of the three methods with CPW = 37.1 and CFLN = 3.4647 in the nonuniform grid system.**

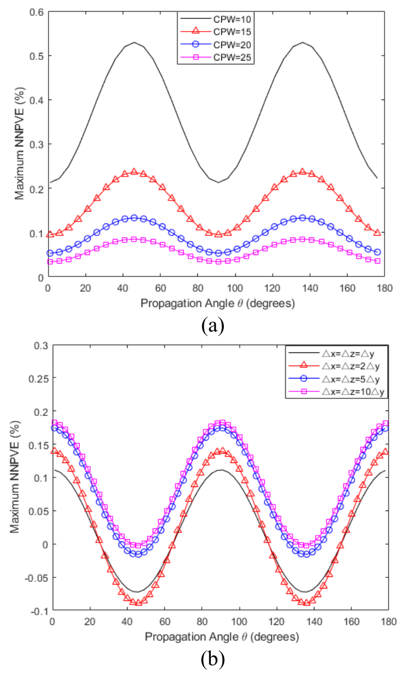

FIGURE 5. **The maximum NNPVE of the AA four-step HIE-FDTD method versus θ with different (a) CPW; (b) grid sizes.**

HIE-FDTD method is only 0.02486%, achieving significant optimization. (3) When CFLN = 1.1547, the AA four-step HIE-FDTD method remains stable, thus, the weak stability condition has been proven.

Figs. 3 and 4 are the numerical dispersion characteristics analysis of the proposed method in the nonuniform grid system. The grid system having a fine structure in the y-direction is assumed here, $\Delta x = \Delta z = 5\Delta y = \lambda/37.1$, that is, CPW = 37.1, and CFLN = 3.4647. The AA parameters of the proposed method can be obtained as $\varepsilon_x = \varepsilon_z = 0.9992$ and $\varepsilon_y = 0.9999$.

Fig. 3 discusses Maximum NNPVE versus θ of the six methods. Fig. 4 shows the comparison of the NNPVE versus θ and φ for the FDTD method, the four-step HIE-FDTD method before and after optimization. The following conclusions can be obtained from Figs. 3 and 4. (1) When CFLN = 3.4647, the AA four-step HIE-FDTD method is stable and has a lower NNPVE value, indicating that the proposed method is weak conditionally stable in the nonuniform grid system. (2) Among the six FDTD methods, the maximum NNPVE value of the AA four-step HIE-FDTD method is smallest, even lower than that of the traditional FDTD algorithm.

Fig. 5 analyzes the effect of different indicators on the dispersion characteristics of the AA four-step HIE-FDTD method. Fig. 5(a) is a comparison of the maximum NNPVE when CPW = 10, 15, 20 and 25, respectively, and CFLN = 10 in the 5 times nonuniform grid system ($\Delta x = 5\Delta y = \Delta z$). As can be seen from Fig. 5(a), when CPW = 10, the maximum NNPVE of the proposed method is the largest, and the maximum NNPVE value is 0.5292% at $\theta = 45°$; when CPW = 15, the maximum NNPVE value of the proposed method is 0.2363%, which is lower than that of CPW = 10; when CPW = 25, the maximum NNPVE of the proposed method is the smallest, which is only 0.08528% at $\theta = 45°$. In Fig. 5(b), CFLN = 2, CPW = 15, and the four curves represent the maximum NNPVE of the AA

TABLE 1. A comparison of the results for uniform grids

Methods	CFLN	Step Number	CPU Times (s)	Result（GHz） TE_{011} (26.926)	Relative Error（%）
FDTD	0.5	24000	34	26.90	0.097
Four-step HIE-FDTD	3	4000	36	26.86	0.245
AA four-step HIE-FDTD	3	4000	37	26.93	0.015

four-step HIE-FDTD method versus θ when the grid size is $\Delta x = \Delta z = (1, 2, 5, 10)\Delta y$. It can be seen from Fig. 5(b), the maximum NNPVE of the proposed method decreases as the increase of the nonuniform multiple with θ in the range of [36°, 144°]. Accordingly, it can be inferred that the finer the spatial meshing, the smaller the numerical dispersion error of the proposed method.

V. NUMERICAL RESULT

In this section, in order to verify the computational efficiency and accuracy of the proposed method, a 3-D cavity with the size of 9 mm × 6 mm × 15 mm is simulated. The performances of the AA four-step HIE method and the four-step HIE-FDTD method are compared, and the traditional FDTD method is used as a reference. A sinusoidal modulated Gaussian pulse source with the expression of $exp[-(t-t_0)2/T^2] \times sin[2\pi f_0(t-t_0)]$ is placed at the center of the cavity, where $T = 30$ ps, $t_0 = 3 \times T$, and $f_0 = 20$ GHz. The observation point is located at 4.2 mm from the center point along the x-axis. In the simulation, both uniform grid system and five times nonuniform grid system are used. In addition, the coarse grid and fine grid are used in the nonuniform grid system.

Fig. 6 and Table 1 show the simulation results of the three FDTD methods in a uniform grid system. The grid size is $\Delta x = \Delta y = \Delta z = 0.3$ mm, and corresponding number of grids is 30 × 20 × 50. For the FDTD method, CFLN = 0.5, and the step number is 24000. The other two four-step HIE-FDTD methods with CFLN = 3, the step number is 4000, and the total simulation time is selected to be 6.888 ns. The optimization parameters of the AA four-step HIE-FDTD method are set as $\varepsilon_x = \varepsilon_z = 0.99701$ and $\varepsilon_y = 0.99970$.

It can be seen from Fig. 6(a) that the simulation results of the three FDTD methods are basically coincident and stable, while the CFLN of the AA four-step HIE-FDTD method is 3, this verifies the weak conditional stability of the proposed method in a uniform grid system.

From Fig. 6(b) and Table 1, it can be seen that among the three FDTD methods, the resonant frequency calculated by the AA four-step HIE-FDTD method is closest to the theoretical value, and the relative error is the smallest, only 0.015%, which is much smaller than that of the four-step HIE-FDTD (the relative error of 0.245%) and the traditional FDTD method (the relative error of 0.097%). It shows that

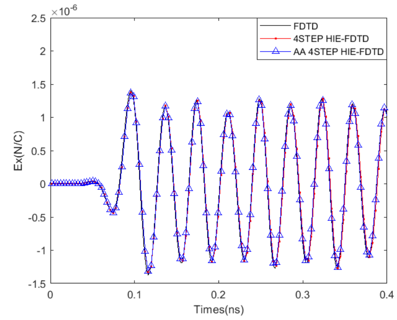

(a)

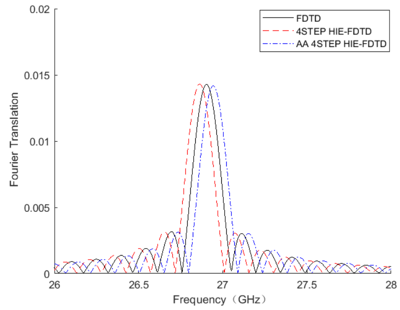

(b)

FIGURE 6. Simulation results in uniform grid system with CFLN = 0.5 for the FDTD method and CFLN = 3 for the two HIE-FDTD methods. (a) E_x; (b) resonant frequency.

the AA four-step HIE-FDTD method has the high calculation accuracy, and it proves that the effect of optimization on the AA four-step HIE-FDTD method is very obvious. Furthermore, from Table 1, it is observed that the CPU time of the AA four-step HIE-FDTD method is similar to that of the four-step HIE-FDTD method, whereas the computational accuracy of the proposed method is high than that of the four-step HIE-FDTD method.

Fig. 7 shows the simulation results of the time-domain electric field E_x and the resonant frequency using three methods in a nonuniform fine grid system. The grid size is $\Delta x = 5\Delta y = \Delta z = 0.3$ mm, and corresponding number of grids is 30 × 100 × 50. The FDTD method takes CFLN = 1, the step number is 15000, and the other two four-step HIE-FDTD methods take CFLN = 10, the step number is 1500, and the total simulation time is 5.772 ns. The optimization parameters of the AA four-step HIE-FDTD method are $\varepsilon_x = \varepsilon_z = 0.99789$, $\varepsilon_y = 1.00007$.

It can be seen from Fig. 7 that, the simulation results of the three methods are basically coincident with each other, which proves the weak conditional stability of the AA four-step HIE-FDTD method in the nonuniform grid system.

Table 2 presents the comparison of the results for three methods using a coarse grid and a fine grid in a nonuniform grid system. The grid size of the fine grid is $\Delta x = 5\Delta y = \Delta z = 0.3$ mm, which is consistent with the grid in Fig. 7, and in the coarse grid, the grid size is $\Delta x = 5\Delta y = \Delta z = 0.6$ mm, and the number of grids is 15 × 50 × 25. In addition, the FDTD method takes CFLN = 1, and the step number is 15000. The other two four-step HIE-FDTD methods take CFLN = 10, the step number of the simulation is 1500, and

TABLE 2. A comparison of the results for nonuniform grids

Methods	CFLN	Grid size: $\Delta x = 5\Delta y = \Delta z = 0.6mm$				Grid size: $\Delta x = 5\Delta y = \Delta z = 0.3mm$			
		Step Number	CPU Times (s)	Result (GHz) TE_{011}(26.926)	Relative Error (%)	Step Number	CPU Times(s)	Result (GHz) TE_{011}(26.926)	Relative Error（%）
FDTD	1	15000	14	26.92	0.0223	30000	216	26.92	0.0223
Four-step HIE-FDTD	10	1500	8	26.73	0.7279	3000	156	26.87	0.2080
AA four-step HIE-FDTD	10	1500	8	26.92	0.0223	3000	165	26.92	0.0223

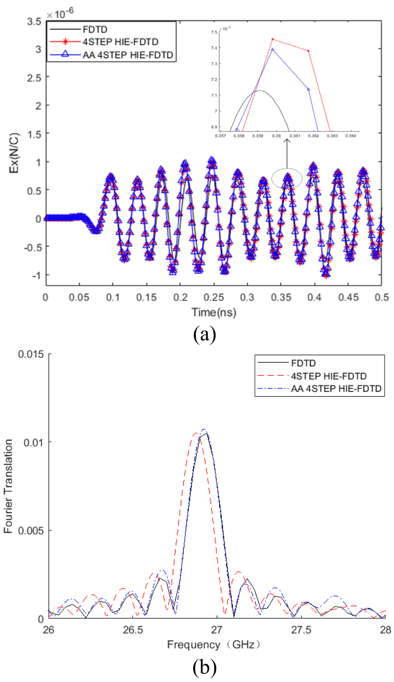

FIGURE 7. Simulation results in nonuniform grid system with CFLN = 1 for the FDTD method and CFLN = 10 for the two HIE-FDTD methods. (a) E_x; (b) resonant frequency.

the total simulation time is 5.772 ns. For the AA four-step HIE-FDTD algorithm, the optimization parameters in the fine grid and coarse grid are $\varepsilon_x = \varepsilon_z = 0.99789$, $\varepsilon_y = 1.00007$, and $\varepsilon_x = \varepsilon_z = 1.00026$, $\varepsilon_y = 0.99161$, respectively.

For the fine grid, it can be observed from Table 2 that, when CFLN = 10, the relative error of the resonant frequency calculated by the four-step HIE-FDTD method is 0.2080%, whereas that of the AA four-step HIE-FDTD method is only 0.0223%, which is the same as that of the FDTD method with CFLN = 1. Therefore, compared with the four-step HIE-FDTD method, the calculation accuracy of the proposed method has been proven. Furthermore, the CPU time of the FDTD, the four-step HIE-FDTD method and the AA four-step HIE-FDTD method are 216 s,156 s,165 s, respectively. In other words, with the same level of accuracy, the CPU time of the AA four-step HIE-FDTD is reduced 51s compared with the FDTD method, and the computational efficiency of the proposed method can be improved. For the two four-step HIE-FDTD methods, it is obvious that the influence of the instruction of the AA parameters for the CPU time is not remarkable.

Further observation of Table 2 shows that the relative error of the four-step HIE-FDTD method in the coarse grid is more than that of result in the fine grid, whereas the relative error of the AA four-step HIE-FDTD method remains small. The effect on the optimization for the AA four-step HIE-FDTD method is further proved, and the AA four-step HIE-FDTD method has higher computational accuracy. Furthermore, the AA four-step HIE-FDTD method and the FDTD method have the same level of accuracy, and the CPU time are 14 s and 8 s, respectively. Therefore, the AA four-step HIE-FDTD method is more efficient than the FDTD method.

VI. CONCLUSION

In this article, by introducing artificial anisotropy parameters, the AA four-step HIE-FDTD method has been proposed to reduce the numerical dispersion error. Firstly, artificial anisotropy parameters are introduced in the four-step HIE-FDTD method to obtain the basic formulation of the AA four-step HIE-FDTD method. Secondly, the CFL stability condition of the proposed method is discussed, which is basically consistent with that of the four-step HIE-FDTD method. Thirdly, the numerical dispersion characteristics of the proposed method are analyzed, and compared with other methods for case of the CPW value, the CFLN value and the nonuniform multiple. It is theoretically proved that the presented method has a lower numerical dispersion error. Finally, to verify the computational accuracy and efficiency of the proposed method, numerical simulation results are also performed. The simulation results show that, compared with the pre-optimization, the AA four-step HIE-FDTD method has higher calculation accuracy, and compared with the traditional FDTD method, it has higher computational efficiency with the same level of accuracy.

REFERENCES

[1] K. Yee, "Numerical solution of initial boundary value problems involving Maxwell's equations in isotropic media," *IEEE Trans. Antennas Propag.*, vol. AP-14, no. 3, pp. 302–307, May 1966.

[2] A. Taflove and S. C. Hagness, *Computational Electrodynamics: The Finite-Difference Time-Domain Method*, 2nd ed. Boston, MA, USA: Artech House, 2000.

[3] T. Namiki, "A new FDTD algorithm based on alternating-direction implicit method," *IEEE Trans. Microw. Theory Techn.*, vol. 47, no. 10, pp. 2003–2007, Oct. 1999.

[4] F. Zhen, Z. Chen, and J. Zhang, "Toward the development of a three-dimensional unconditionally stable finite-difference time-domain method," *IEEE Trans. Microw. Theory Techn.*, vol. 48, no. 9, pp. 1550–1558, Sep. 2000.

[5] G. Sun and C. W. Trueman, "Efficient implementations of the Crank-Nicolson scheme for the finite-difference time-domain method," *IEEE Trans. Microw. Theory Techn.*, vol. 54, no. 5, pp. 2275–2284, May 2006.

[6] J. Lee and B. Fornberg, "A split step approaches for the 3-D Maxwell's equations," *J. Comput. Appl.*, vol. 158, no. 2, pp. 485–505, 2003.

[7] W. Fu and E. L. Tan, "Development of split-step FDTD method with higher-order spatial accuracy," *Electron. Lett.*, vol. 40, no. 20, pp. 1252–1253, Sep. 2004.

[8] Y.-D. Kong and Q.-X. Chu, "High-order split-step unconditionally-stable FDTD methods and numerical analysis," *IEEE Trans. Antennas Propag.*, vol. 59, no. 9, pp. 3280–3289, Sep. 2011.

[9] J. Shibayama, M. Muraki, J. Yamauchi, and H. Nakano, "Efficient implicit FDTD algorithm based on locally one-dimensional scheme," *Electron. Lett.*, vol. 41, no. 19, pp. 1046–1047, Sep. 2005.

[10] I. Ahmed, E.-K. Chua, E.-P. Li, and Z. Chen, "Development of the three-dimensional unconditionally stable LOD-FDTD method," *IEEE Trans. Antennas Propag.*, vol. 56, no. 11, pp. 3596–3600, Nov. 2008.

[11] A. K. Saxena and K. V. Srivastava, "A three-dimensional unconditionally stable five-step LOD-FDTD method," *IEEE Trans. Antennas Propag.*, vol. 62, no. 3, pp. 1321–1329, Mar. 2014.

[12] B. Huang, G. Wang, Y. Jiang, and W. Wang, "A hybrid implicit-explicit FDTD scheme with weakly conditional stability," *Microw. Opt. Technol. Lett.*, vol. 39, no. 2, pp. 97–101, Oct. 2003.

[13] J. Chen and J. Wang, "A 3D hybrid implicit-explicit FDTD scheme with weakly conditional stability," *Microw. Opt. Technol. Lett.*, vol. 48, no. 11, pp. 2291–2294, Nov. 2006.

[14] J. Chen and J. Wang, "A novel WCS-FDTD method with weakly conditional stability," *IEEE Trans. Electromagn. Compat.*, vol. 49, no. 2, pp. 419–426, May 2007.

[15] Q. Zhang, B. Zhou, and J. B. Wang, "A novel hybrid implicit-explicit FDTD algorithm with more relaxed stability condition," *IEEE Antennas Wireless Propag. Lett.*, vol. 12, pp. 1372–1375, 2013.

[16] Q. Zhang and B. H. Zhou, "A novel HIE-FDTD method with large time-step size," *IEEE Antennas Propag Magaz.*, vol. 57, no. 2, pp. 24–28, Apr. 2015.

[17] J. Wang, B. Zhou, L. Shi, C. Gao, and B. Chen, "A novel 3-D HIE-FDTD method with one-step leapfrog scheme," *IEEE Trans. Microw. Theory Techn.*, vol. 62, no. 6, pp. 1275–1283, Jun. 2014.

[18] J. Wang, J. Wang, B. Zhou, and C. Gao, "An efficient 3-D HIE-FDTD method with weaker stability condition," *IEEE Trans. Antennas Propag.*, vol. 64, no. 3, pp. 998–1004, Mar. 2016.

[19] Y.-D. Kong, C.-B. Zhang, M. Lai, and Q.-X. Chu, "A novel four-step weakly conditionally stable hie-FDTD algorithm and numerical analysis," *Prog. Electromagn. Res. M*, vol. 82, pp. 183–194, 2019.

[20] J. S. Juntunen and T. D. Tsiboukis, "Reduction of numerical dispersion in FDTD method through artificial anisotropy," *IEEE Trans. Microw. Theory Techn.*, vol. 48, no. 4, pp. 582–588, Apr. 2000.

[21] H.-X. Zheng and K. Wa Leung, "An efficient method to reduce the numerical dispersion in the ADI-FDTD," *IEEE Trans. Microw. Theory Techn.*, vol. 53, no. 7, pp. 2295–2301, Jul. 2005.

[22] Y. Zhang, S. W. Lü, and J. Zhang, "Reduction of numerical dispersion of 3-D higher order alternating-direction-implicit finite difference time-domain method with artificial anisotropy," *IEEE Trans. Microw. Theory Techn.*, vol. 57, no. 10, pp. 2416–2428, Oct. 2009.

[23] K. Niu, Z. Huang, M. Li, and X. Wu, "Optimization of the artificially anisotropic parameters in WCS-FDTD method for reducing numerical dispersion," *IEEE Trans. Antennas Propag.*, vol. 65, no. 12, pp. 7389–7394, Dec. 2017.

[24] Q. Lei, J. Wang, L. Shi, and H. Chen, "Improved artificial anisotropy HIE FDTD algorithm for periodic structures at oblique incidence," *IEEE Trans. Antennas Propag.*, vol. 65, no. 12, pp. 7395–7398, Dec. 2017.

[25] K. K. Niu, Z. X. Huang, B. Wu, and X. L. Wu, "3D optimised hybrid implicit-explicit FDTD method with suppressed numerical dispersion," *Electron. Lett.*, vol. 54, no. 6, pp. 335–336, Mar. 2018.

[26] Y.-D. Kong, C.-B. Zhang, and Q.-X. Chu, "An optimized one-step leapfrog HIE-FDTD method with the artificial anisotropy parameters," *IEEE Trans. Antennas Propag.*, vol. 68, no. 2, pp. 1198–1203, Feb. 2020.

YONG-DAN KONG (Member, IEEE) was born in Heze, Shandong, China, in 1981. She received the Ph.D. degree in electronic and information engineering from the South China University of Technology, Guangzhou, Guangdong, China, in 2011. She is currently an Associate Professor with the South China University of Technology. Her current research interest includes computational electromagnetics and antenna.

CHU-BIN ZHANG was born in Shaoyang, Hunan, China, in 1994. She received the B.S. degree in communication engineering from Lanzhou University, Lanzhou, China, in 2016, and the M.S. degree in electromagnetic field and microwave technology from the South China University of Technology, Guangzhou, China, in 2019.

Her current research interest includes unconditionally-stable finite-difference time-do main (FDTD) method.

HONG-YU ZHANG was born in Jingzhou, Hubei, China, in 1998. She received the B.S. degree in communication engineering from Fujian Normal University, Fujian, China, in 2019. She is currently pursuing the M.S. degree in electromagnetic field and microwave technology from the South China University of Technology, Guangzhou, China.

Her current research interest includes conditionally-stable finite-difference time-domain (FDTD) method.

QING-XIN CHU (Fellow, IEEE) received the B.S., M.E., and Ph.D. degrees in electronic engineering from Xidian University, Xi'an, Shaanxi, China, in 1982, 1987, and 1994, respectively.

From January 1982 to January 2004, he was with the School of Electronic Engineering, Xidian University, where he has been a Professor and the Vice Dean of the School of Electronic Engineering, since 1997. Since 2011, he has been a Distinguished Professor with Xidian University in Shaanxi Hundred-Talent Program. He is currently a Chair Professor with the School of Electronic and Information Engineering, South China University of Technology, where he is also the Director of the Research Institute of Antennas and RF Techniques and also the Chair of the Engineering Center of Antennas and RF Techniques of Guangdong Province. He has published more than 300 articles in journals and conferences, which were indexed in SCI more than 1500 times. One of his papers published in the IEEE Transactions on Antennas and Propagations, in 2008, becomes the top ESI (Essential Science Indicators) article within 10 years in the field of antenna (SCI indexed self-excluded in the antenna field ranged top 1%). He has authorized more than 30 invention patents of China. In 2014, he was elected as the highly cited scholar by Elsevier in the field of Electrical and Electronic Engineering. His current research interests include antennas in wireless communication, microwave filters, spatial power combining array, and numerical techniques in electromagnetics.

Dr. Chu is the Senior Member of the China Electronic Institute (CEI). He was a recipient of the Science Awards by the Education Ministry of China, in 2002 and 2008, the Singapore Tan Chin Tuan Exchange Fellowship Award, in 2003, the Educational Award by Shaanxi Province, in 2003, the Fellowship Award by the Japan Society for Promotion of Science (JSPS), in 2004, and the Science Award by Guangdong Province, in 2013. He is the Foundation Chair of the IEEE Guangzhou AP/MTT Chapter.